Comparative Study of Contrast Enhancement and Illumination Equalization Methods for Retinal Vasculature Segmentation

Aliaa A. A. Youssif, Atef Z. Ghalwash, and Amr S. Ghoneim
Faculty of Computers and Information, Helwan University, Cairo, Egypt
e-mail: aliaay@yahoo.com, aghalwash@edara.gov.eg, amr_ghoneim@yahoo.com

***Abstract*—Retinal vasculature segmentation is a main step while developing automated screening systems for diabetic retinopathy. Digital fundus images are routinely analyzed by screening systems, and owing to the acquisition process, these images are very often of poor quality that hinders further analysis. Uneven illumination and contrast variability throughout the image significantly affect the vessels segmentation process. State-of-the-art studies still struggle with the issue of normalizing contrast and illumination in retinal images, mainly due to the lack of literature reviews and comparative studies. Furthermore, available normalization methods are not being evaluated on large benchmark publicly-available datasets. The paper discusses eight contrast enhancement and illumination equalization methods described in literature. A comparative performance measure based on a simple standard vessel segmentation algorithm is accomplished among available methods, using two publicly-available fundus datasets. Moreover, when applying a local contrast enhancement proceeded by an illumination equalization method to fundus images, a noticeable enhancement in the vasculature segmentation was achieved.**

***Index Terms*—Biomedical image processing, comparative study, fundus image analysis, normalization, retinal imaging, telemedicine, vessel segmentation.**

I. Introduction

SEGMENTATION of the retinal vasculature (RV) in digital fundus images is a key step in automatic screening systems for diabetic retinopathy (DR); one of the most prevalent complications of diabetes [1], and the leading cause of blindness in the Western World [2]. The RV serves as a landmark for other fundus features, such as the optic disc [3]–[5]. In addition, RV segmentation is required to stop the curvilinear shapes from interfering with later analysis of DR lesions [6], and to assist ophthalmologists by parameters such as vessel tortuosity. Moreover, RV can possibly be used as an indicator of the state of the cerebral vasculature, assisting the detection of cerebral microvascular changes in aging, as well as diseases such as vascular dementia and stroke [7].

In General, retinal photography is significantly more effective than direct ophthalmoscopy in detecting DR [8]. Digital fundus images are more appropriate for automatic screening systems since they don't require the injection of fluorescein or indocyanine green dye into the body, and with the availability of non-mydriatic digital color fundus cameras *(i.e. that do not require pupil dilation)*.

Unfortunately, significant percentage of retinal fundus images are of poor quality that hinders analysis due to many factors such as patient movement, poor focus, bad positioning, reflections, disease opacity, or inadequate illumination [6]. Besides, the improper focusing of light may radially decrease the brightness of the image outward from the center, leading to sort of uneven illumination known as vignetting [3], which consequently affects the contrast throughout the image.

These artifacts are significant enough to impede human grading and automated analysis in about 15% of retinal images [6], [9]. Preprocessing steps can wilt or even remove the mentioned interferences, and are a necessary pre-requisite to obtain images with normalized values for luminosity and contrast. Though [10] is a published study that compares the performance of various normalization methods, these methods have not been evaluated on large publicly available benchmark datasets, such as [11] and [12].

The remaining part of the paper is organized as follows. Illumination equalization and contrast enhancement methods proposed in literature for the specific application to retinal fundus images are reviewed in Section II. In Section III, a description of the material used is given. Section IV presents the results of the comparative study. Finally, Section V discusses and summarizes the given results.

II. Methods: A Literature Review

The illumination in a retinal image is non-uniform due to the variation of the retina response or the non-uniformity of the imaging system *(e.g. vignetting, and varying the eye position relative to the camera)*. Vignetting and other forms of uneven illumination make the typical analysis of retinal images impractical and useless. Consequently, the contrast within the image is affected, and needs to be enhanced so that the result is more appropriate for the application of automatic vessels segmentation algorithms. Sinthanayothin [13] defined contrast enhancement by *'any process that expands the range of the significant intensities'*. Contrast enhancement techniques vary in how the major range of intensities is identified and expanded [13]. Several techniques have been used to improve uneven luminosity and contrast levels.

1) Green Band Processing: In order to simply enhance the contrast of the retinal fundus images, some information is commonly discarded before processing, such as the red *(so-called red-free images)* and blue components of the image. Consequently, only the green band is extensively used in the processing as it displays the best vessels/background contrast [14], and the greatest contrast between the optic disk and the retinal tissue [15]. In addition, micro-aneurysms *(a diabetic retinopathy early symptom)* are more distinguishable from the background in the green band although they normally appear as small reddish spots on the retina [16]. Conversely, the red and the blue bands are hardly used by automated applications. Therefore, many vessel detection and optic disc localization

methods are based on the green component of the color fundus image [14]–[17].

2) Histogram Equalization: A typical well-known technique for contrast enhancement which spans the histogram of an image to a fuller range of the gray scale [18]. The histogram of a digital image with *L* total possible intensity levels is defined as the discrete function:

$$h(r_k) = n_k \qquad k = 0, 1, 2, \ldots, L-1 \tag{1}$$

where r_k is the *k*th intensity level in the given interval and n_k is the number of pixels in the image whose intensity level is r_k [19]. Thus, a histogram equalized image is obtained by mapping each pixel with level r_k in the input image to a corresponding pixel with level s_k in the output image using the following equation *(based on the cumulative distribution function 'CDF')*:

$$s_k = T(r_k) = \sum_{j=0}^{k} p_r(r_j) = \sum_{j=0}^{k} n_j / n \qquad k = 0, 1, 2, \ldots, L-1 \tag{2}$$

where $p_r(r_j)$ is the probability of occurrence of gray level r_j in an image *(i.e. the probability density function 'PDF')*, and *n* is the total number of pixels in the image.

Although histogram equalization is a standard technique, it has drawbacks since it depends on the global statistics of an image. For instance, a washed-out appearance can be seen in parts of the image due to over enhancement, while other parts need more enhancing such as the peripheral region [13], [18].

3) Adaptive Local Contrast Enhancement: A technique invented by Sinthanayothin *et al.* [13] in which it does not depend on the global statistics of the image. Instead, it is applied to local areas depending on its mean and variance. Considering a window '*W*' of size *M*×*M (empirically, M = 49)*, centered on the pixel (i, j), then the pixel is altered by:

$$f(i, j) = 255 * \left[\frac{\left[\Psi_W(f) - \Psi_W(f_{\min})\right]}{\left[\Psi_W(f_{\max}) - \Psi_W(f_{\min})\right]} \right] \tag{3}$$

where $f_{\min}$ and $f_{\max}$ are the minimum and maximum intensities in the whole image, and the sigmoidal function $\Psi_W(f)$ is:

$$\Psi_W(f) = \left[1 + \exp\left(\frac{< f >_W - f}{\sigma_W} \right) \right]^{-1} \tag{4}$$

where $< f >_W$ and σ_W are respectively the mean and variance of the intensities within *W*. It is recommended to apply a 2D-Gaussian/median filter to the image before enhancement to reduce enhanced noise within the image [20].

4) Adaptive Histogram Equalization (AHE): A method applied by Wu *et al.* [21], and was found more effective than the classical histogram equalization when considering the detection of small blood vessels characterized by low contrast levels and intensities that decline significantly with the reduction of the vessels' width. To apply the AHE to an intensity image *I*, each pixel *p* in the image is adapted using the following equation:

$$I_{AHE}(p) = \left(\sum_{p' \in R(p)} s(I(p) - I(p')) / h^2 \right)^r * M \tag{5}$$

where $M = 255$, $R(p)$ denotes the pixel *p*'s neighborhood (a square window with length *h)*, $s(d) = 1$ if $d > 0$ and $s(d) = 0$ otherwise. The values of *h* and *r* where empirically chosen to be 81 and 8 respectively. In [21], the AHE was applied to an illumination equalized inverted green band.

5) Desired Average Intensity: To overcome the non-uniform illumination, Hoover and Goldbaum [3] adjusted *(equalized)* each pixel using the following equation:

$$I_{eq}(r, c) = I(r, c) + m - \bar{I}_W(r, c) \tag{6}$$

where *m* is the desired average intensity *(128 in an 8-bit grayscale image)* and $\bar{I}_W(r, c)$ is the mean intensity value of the pixels within a window *W* of size *N*×*N*. The mean intensities are smoothed using the same windowing. The window size *N* applied by [3] was variable *(between 30 and 50)* in order to use the same number of pixels every time while computing the average at the center or near the border.

In [4], a running window of only one size *(40×40)* was used to calculate the mean intensity value using (6), thus the amount of pixels used while calculating the local average intensity in the center is more than the amount of pixels used near the border. Although the resulting images look very similar to those using the variable running window, the ROI of the retinal images is shrunk by five pixels to discard the pixels near the border where the chances of erroneous values are higher [4].

6) Division by an Over-Smoothed version: In [16], Yang *et al.* corrected the non-uniform illumination by dividing the image by an over-smoothed version of it using a spatially large median filter. Usually, the illumination equalization process is applied to the green band *(green image)* of the retina [3], [4], and [16].

7) Background Subtraction of Retinal Blood Vessels (BSRBV): A method proposed by Lin and Zheng [22] to enhance the RV by subtracting the non-stationary background. The fundus image was modeled as having two components: the blood vessels (foreground) and the background which was estimated by averaging the neighborhood (local) intensity to suppress the vessels. The estimated background component was subsequently smoothed by threshold averaging (using the minimum of local average values from the images' four corner). Then finally, it was subtracted from the original image resulting in an enhanced image, free from background interference, thus suitable for later segmentation.

8) Estimation of Background Luminosity and Contrast Variability (EBLCV): In order to normalize the illumination and contrast in retinal images, Foracchia *et al.* [10] used the same foreground-background model proposed by [22]. The non-uniform contrast and luminosity imposed by an acquisition model $f(\cdot)$ to the original image I°, resulting in the observed image I can be described as follows:

$$I(x, y) = f(I^\circ(x, y)) = C(x, y) I^\circ(x, y) + L(x, y) \tag{7}$$

where C and L are respectively the contrast and luminosity drift factors.

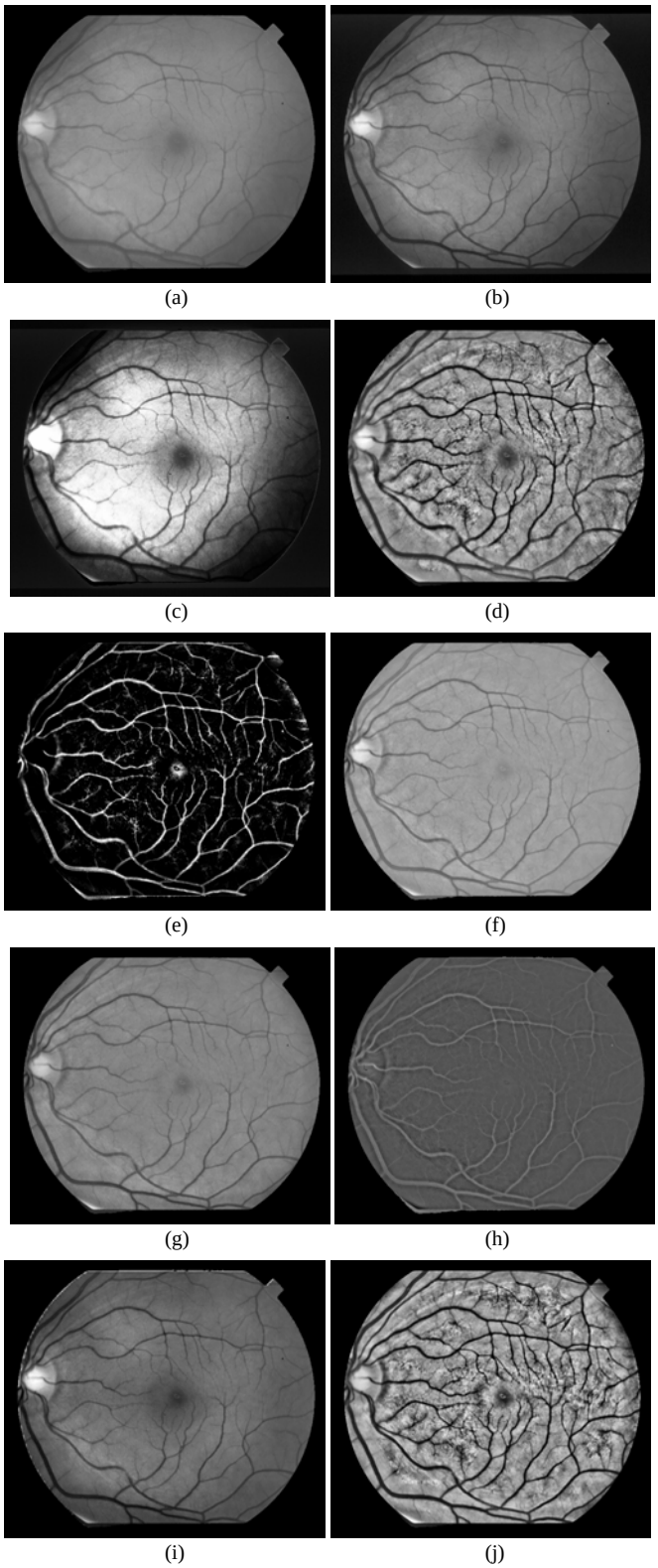

Fig.1 Reviewed normalizations of a typical fundus image. (a) Intensity image. (b) Green-band image. (c) Histogram equalization. (d) Adaptive local contrast enhancement. (e) Adaptive histogram equalization. (f) Desired average intensity. (g) Division by an over-smoothed version. (h) Background subtraction of retinal blood vessels. (i) Estimation of background luminosity and contrast variability. (j) Adaptive local contrast enhancement applied to 'g' instead of 'a'.

Therefore, an estimate $\hat{I}^{\circ}$ of the original image was recovered using the following equation:

$$\hat{I}^{\circ}(x,y) = \frac{I(x,y) - \hat{L}(x,y)}{\hat{C}(x,y)} \tag{8}$$

where $\hat{C}$ and $\hat{L}$ are the estimation of C and L. In order to extract the background pixels, the mean and standard deviation were calculated in the neighborhood N of each pixel, and then the Mahalanobis distance from the mean was used to mark pixels as background using a threshold value set to 1. The luminosity and contrast drifts were then estimated by calculating the mean and standard deviation for the background pixels in N. Finally, given the observed image, the original image can be recovered using (8).

III. Material

Two publicly available datasets were used. The first one is the DRIVE dataset [11], established to facilitate comparative studies on RV segmentation [2], [23]. The dataset consists of a total of 40 color fundus photographs used for making actual clinical diagnoses, and divided into 2 equal sets *(training and test)*, where 33 photographs do not show any sign of diabetic retinopathy and 7 show signs of mild early diabetic retinopathy. The – *24 bits, 768 by 584 pixels* – color images are in compressed JPEG-format, commonly used in screening. They were acquired using a Canon CR5 non-mydriatic 3CCD camera with a 45 degree field-of-view (FOV). A manually thresholded FOV is included for each image beside a manual segmentation of the vasculature for the training set, and two manual segmentations for the test set [2].

The second dataset used is a subset of the STARE Project's dataset [12], containing 20 fundus images used by Hoover *et al.* [24] for testing an automated vessel segmentation method, with two manual segmentations available (Fig. 2(k)). The images were captured using a TopCon TRV-50 fundus camera at 35° FOV, and subsequently digitized at 605 x 700, 24-bits pixel [24]. Ten of the images are of patients with no pathology while the other ten images contain pathology that obscures or confuses the RV appearance in varying portions of the image.

IV. Results

Instead of applying the adaptive local contrast enhancement to the intensity image as proposed by [13], we applied it to the illumination equalized image obtained by [16] using division by an over-smoothed version. In order to compare the eight reviewed normalization methods (Fig. 1 (a)-(i)), and the proposed hybrid method (Fig. 1 (j)), a vessel segmentation algorithm [17] is applied to the 60 images *(before and after applying each of the normalization methods)*, (Fig. 2 (a) (j)).

The publicly available manual RV segmentations were used as our gold standard. The intensity image represents a normal gray-level image before enhancement. The adaptive histogram equalization, and the BSRBV methods were applied to an inverted green band image, thus both methods used an

inverted version of the 2D matched filters used for segmentation [17].

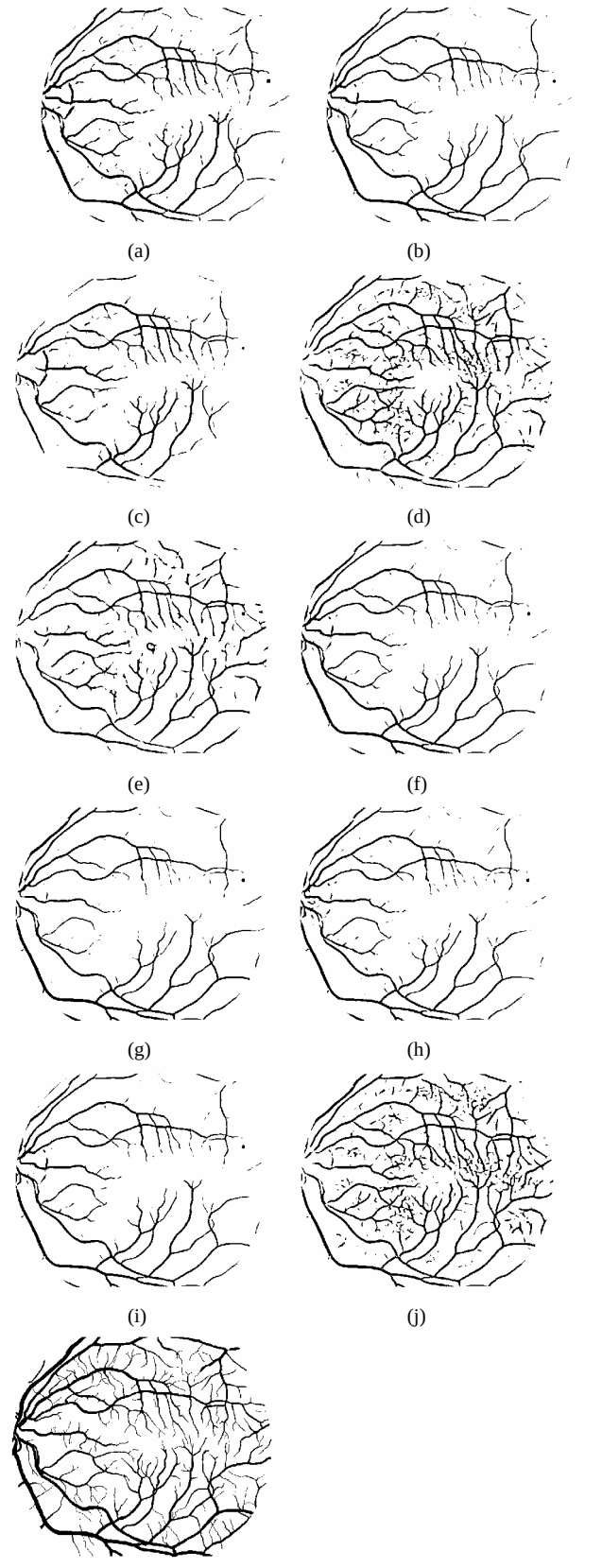

Fig.2 (a)-(i) are the results of applying a RV segmentation method to the images *Fig. 1 (a)-(j)* respectively. (k) A manual segmentation of *Fig. 1 (a)* (used as a gold-standard).

The EBLCV was applied using *201×201* tessellated windows [10], and then full images were approximated using bicubic interpolation. For evaluating the performance of the normalization methods, we used the receiver operating characteristic (ROC) curve [25] (Fig. 3). The area under the ROC curve was calculated using a non-parametric estimate [26] to measure the overall performance as shown in Table I.

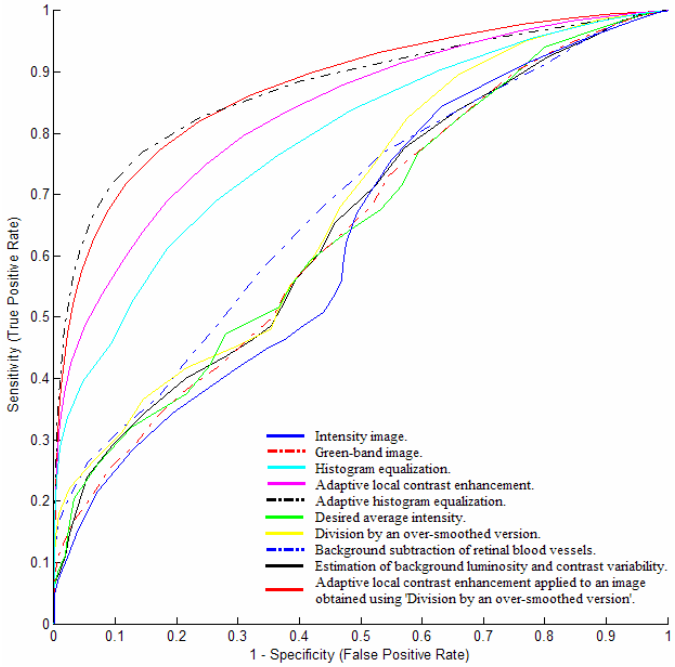

Fig.3 ROC curves of the compared normalization methods.

TABLE I
AREA UNDER CURVE (AUC) MEASURED PER NORMALIZATION METHOD

Normalization Methods	AUC
Intensity image	0.629
Green band image	0.641
Histogram equalization	0.787
Adaptive local contrast enhancement	0.833
Adaptive histogram equalization	0.874
Desired average intensity	0.646
Division by an over-smoothed version	0.676
Background subtraction of retinal blood vessels	0.677
Estimation of background luminosity and contrast variability	0.650
Adaptive local contrast enhancement applied to the illumination equalized image obtained using division by an over-smoothed version	0.876

V. DISCUSSION AND CONCLUSION

The paper presented and compared nine different methods for contrast enhancement and illumination equalization of retinal fundus images. Two publicly available databases of total 60 images along with a simple vasculature segmentation algorithm were used for the test purpose.

The adaptive histogram equalization was found to be the most effective method as it obviously improved the segmentation algorithm, thus it attained the largest area under the ROC curve. The adaptive local contrast enhancement and the typical histogram equalization methods recorded

respectively the second and third best results, noticeably improving the RV segmentation algorithm. In general, the three mentioned methods reasonably improved and normalized the contrast and illumination throughout the images, while the remaining methods attained a poor performance although they have almost increased the AUC. Applying the adaptive local contrast enhancement to an illumination equalized image further enhanced the results, and achieved better results than being applied to the intensity component of an image as proposed in [13].

An extension for this study could be investigating other normalization methods (e.g. [27]–[30]). In addition, more comprehensive results can be achieved by examining the performance of the existing normalization methods using other vasculature segmentation algorithms (e.g. [2], [14], [23] and [24]).

ACKNOWLEDGMENT

The authors wish to thank their fellow authors of references [2], [11]–[13], [17] and [23] for their support in acquiring the materials and resources needed to conduct the present study.

REFERENCES

[1] M. El-Shazly, M. Zeid, and A. Osman, "Risk factors for eye complications in patients with diabetes mellitus: development and progression," *Eastern Mediterranean Health J.*, vol. 6, Issue 2/3, pp. 313-325, 2000.

[2] J. Staal, M. D. Abràmoff, M. Niemeijer, M. A. Viergever, and B. van-Ginneken, "Ridge-based vessel segmentation in color images of the retina," *IEEE Trans. Med. Imag.*, vol. 23, no. 4, pp. 501-509, April 2004.

[3] A. Hoover and M. Goldbaum, "Locating the optic nerve in a retinal image using the fuzzy convergence of the blood vessels," *IEEE Trans. Med. Imag.*, vol. 22, no. 8**,** pp. 951-958, 2003.

[4] Frank ter Haar, "Automatic localization of the optic disc in digital colour images of the human retina," *M.S. Thesis, Utrecht University*, Dec. 16, 2005.

[5] M. Foracchia, E. Grisan, and A. Ruggeri, "Detection of Optic Disc in Retinal Images by Means of a Geometrical Model of Vessel Structure," *IEEE Trans. Med. Imag.*, vol. 23, no. 10, pp. 1189-1195, Oct. 2004.

[6] T. Teng, M. Lefley, and D. Claremont, "Progress towards automated diabetic ocular screening: a review of image analysis and intelligent systems for diabetic retinopathy," *Med. & Biological Engineering & Computing*, vol. 40, pp.2-13, 2002.

[7] N. Patton, T. Aslam, T. MacGillivray, A. Pattie, I. Deary, and B. Dhillon, "Retinal vascular image analysis as a potential screening tool for cerebrovascular disease: a rationale based on homology between cerebral and retinal microvasculatures," *J. Anat.*, vol. 206, no. 4, pp. 319-348, 2005.

[8] S. C. Siu, T. C. Ko, K. W. Wong, and W. N. Chan, "Effectiveness of non-mydriatic retinal photography and direct ophthalmoscopy in detecting diabetic retinopathy," *Hong Kong Med. J.*, vol. 4, no. 4, pp. 367-370, Dec. 1998.

[9] B. Liesenfeld, E. Kohner, W. Piehlmeter, S. Kluthe, S. Aldington, M. Porta, T. Bek, M. Obermaier, H. Mayer, G. Mann, R. Holle, and K-D. Hepp, "A telemedical approach to the screening of diabetic retinopathy: Digital fundus photography," *Diabetes Care*, vol. 23, no. 3, pp.345-348, March 2000.

[10] M. Foracchia, E. Grisan, and A. Ruggeri, "Luminosity and contrast normalization in retinal images," *Medical Image Analysis*, vol. 3, no. 9, pp. 179-190, 2005.

[11] University Medical Center Utrecht, Image Sciences Institute, Research section, Digital Retinal Image for Vessel Extraction (DRIVE) database, [Online]. Available: http://www.isi.uu.nl/Research/Databases/DRIVE

[12] STARE project website. Clemson Univ., Clemson, SC. [Online]. Available: http://www.ces.clemson.edu/~ahoover/stare

[13] C. Sinthanayothin, "Image analysis for automatic diagnosis of diabetic retinopathy," Ph.D. Thesis, University of London (King's College London), September 1999.

[14] D. J. Cornforth, H. J. Jelinek, J. J. G. Leandro, J. V. B. Soares, R. M. Cesar, Jr., M. J. Cree, P. Mitchell, and T. Bossomaier, "Development of retinal blood vessel segmentation methodology using wavelet transforms for assessment of diabetic retinopathy," *8th Asia Pacific Symposium on Intelligent and Evolutionary Systems*, Cairns-Australia, Dec. 6-7, 2004.

[15] R. A. Abdel-Ghafar, T. Morris, T. Ritchings, and I. Wood, "Detection and characterisation of the optic disk in glaucoma and diabetic retinopathy," *Proc. Med. Imag. Understanding and Analysis*, London, Sept. 2004.

[16] G. Yang, L. Gagnon, S. Wang, and M.-C. Boucher, "Algorithm for detecting micro-aneurysms in low-resolution color retinal images," *Proc. Vision Interface 2001*, Ottawa, pp. 265-271, June 7-9, 2001.

[17] S. Chaudhuri, S. Chatterjee, N. Katz, M. Nelson, and M. Goldbaum, "Detection of blood vessels in retinal images using two-dimensional matched filters", *IEEE Trans. Med. Imag.*, vol. 8, no. 3, pp. 263-269, Sept. 1989.

[18] R. C. Gonzalez and R. E. Woods, *Digital Image Processing*, 2nd Ed. Prentice-Hall, 2002.

[19] R. C. Gonzalez, R. E. Woods, and S. L. Eddins, *Digital Image Processing Using MATLAB*, Pearson Education, 2004.

[20] C. Sinthanayothin, J. F. Boyce, H. L. Cook and T. H. Williamson, "Automated localisation of the optic disk, fovea, and retinal blood vessels from digital colour fundus images," *British J. of Ophthalmology*, vol. 83, no. 8, pp.902-910, 1999.

[21] Di Wu, Ming Zhang, Jyh-Charn Liu, and Wendall Bauman, "On the Adaptive Detection of Blood Vessels in Retinal Images," *IEEE Trans. Biomedical Engineering*, vol. 53, Issue: 2, pp: 341-343, Feb. 2006.

[22] Tusheng Lin and Yibin Zheng, "Adaptive image enhancement for retinal blood vessel segmentation," *Electronics Letters*, vol. 38, no. 19, pp. 1090-1091, Sept. 12, 2002.

[23] M. Niemeijer, J. Staal, B. van Ginneken, M. Loog, and M. D. Abràmoff, "Comparative study of retinal vessel segmentation methods on a new publicly available database," in: *SPIE Med. Imag.*, Editor(s): J. Michael Fitzpatrick, M. Sonka, SPIE, vol. 5370, pp. 648-656, 2004.

[24] A. Hoover, V. Kouznetsova, and M. Goldbaum, "Locating blood vessels in retinal images by piecewise threshold probing of a matched filter response," *IEEE Trans. Med. Imag.*, vol. 19, no. 3**,** pp. 203-210, 2000.

[25] Seong Ho Park, Jin Mo Goo, and Chan-Hee Jo, "Receiver Operating Characteristic (ROC) Curve: Practical Review for Radiologists," *Korean J. Radiol.*, vol. 5, pp. 11-18, March 2004.

[26] MedCalc Software, Mariakerke, Belgium, [Online]. Available: http://www.medcalc.be

[27] Øien, G., Osnes, P., "Diabetic retinopathy: automatic detection of early symptoms from retinal images," in: *Proc. NORSIG-95 Norwegian Signal Processing Symposium*, Sept. 1995.

[28] Wang, H., Hsu, W., Goh, K.G., Lee, M.L., "An effective approach to detect lesions in color retinal images," in: *Proc. IEEE Conf. Computer Vision and Pattern Recognition*, vol. 2, pp. 181-186, Jun 2000.

[29] Y. Wang, W. Tan, and S. Lee, "Illumination normalization of retinal images using sampling and interpolation," in: *Med. Imag. 2001: Image Processing. Proc. of SPIE*, vol. 4322, SPIE, pp. 500-507, July 2001.

[30] E. Grisan, A. Giani, E. Ceseracciu, and A. Ruggeri, "Model-based Illumination Correction in Retinal Images," *accepted for publication at the 2006 3rd IEEE International Symposium on Biomed. Imag.*, pp. 984-987, 6-9 April, 2006.